Semi-IPN asymmetric membranes based on polyether imide (ULTEM) and polyethylene glycol diacrylate for gaseous separation

Saimani, Sundar; Kumar, Ashwani

Publisher's version / Version de l'éditeur:
http://dx.doi.org/10.1002/app.28862
Journal of Applied Polymer Science, 110, 6, pp. 3606-3615, 2008

Semi-IPN Asymmetric Membranes Based on Polyether Imide (ULTEM) and Polyethylene Glycol Diacrylate for Gaseous Separation

Sundar Saimani, Ashwani Kumar

National Research Council of Canada, Institute for Chemical Process and Environmental Technology, Montreal Road Campus, Ottawa, Ontario, K1A 0R6, Canada

Received 12 December 2007; accepted 9 June 2008
DOI 10.1002/app.28862
Published online 17 September 2008 in Wiley InterScience (www.interscience.wiley.com).

ABSTRACT: Semi-interpenetrating polymer networks (semi-IPN) formed with commercial polyether imide (ULTEM®, PEI) and poly (ethylene glycol) diacrylate (PEGDA) were used to make asymmetric membranes. The effect of increasing amount of PEGDA on the bulk and the gas separation properties of semi-IPN membranes were studied. The formation of IPNs was confirmed by Fourier Transform Infra Red (FT-IR) spectroscopy. The 5% weight loss temperature decreased and the percent weight loss of the first step increased with increase in the PEGDA content, which indicated the incorporation of more poly (ethylene glycol) (PEG) segments to the semi-IPNs. The microscopic experiments revealed the change in morphology with change in PEGDA content. The Scanning electron micrographs exhibited typical finger-like voids in the sub layer, which is characteristic morphology of asymmetric membranes. The increase in PEGDA content up to 5.7 wt % increased the CO_2/N_2 selectivity of the semi-IPN after which the selectivity decreased and permeance increased. Although, the increase in the polar poly (ethylene glycol) molecules is expected to render better CO_2 selectivity, the performance of the membrane was found to decrease as PEGDA content exceeded 5.7% for the given ratio. J Appl Polym Sci 110: 3606–3615, 2008

Key words: polyether imides; interpenetrating networks; poly (ethylene glycol) diacrylate; gas permeation and plasticization

INTRODUCTION

The separation of gaseous mixtures, in particular CO_2 by polymeric membranes, has gained momentum in recent years, and it progressed from experimental level to industrial products.[1] The market for general polymeric membrane based gas separation products has crossed 150 million/year.[2] The rise in the environmental awareness about the global warming because of green house gas emission has triggered intense research on the carbon-di-oxide capture from industrial flue gases. Number of different polymer membranes have been proposed for the capture of carbon-di-oxide.[3] The main advantages of membrane based separation technology against the conventional absorption, adsorption, and cryogenic distillation techniques are lower energy consumption, lower capital investment, ease of installation and operation, lower maintenance requirements, lower weight and space requirements, and higher process flexibility.[4–6] Although several new polymer materials having higher permeability and selectivity have been reported in the past few years, only very few polymer materials have been used in the commercial products.[1,6] Engineering plastics like polyether imide, polyphenylene oxide and polyether sulfone are widely used as membrane materials in gas separation applications[7–9] because of their high thermal and mechanical stability. Many recent reports described tailor made polymers, but these are often too expensive or complicated to produce on a commercial scale.[3] All the desirable properties for gaseous separation membranes such as good selectivity, permeability, processability, resistant to plasticization, and also inexpensive are difficult to meet with a single polymer. The viable and easy option is to modify the existing polymer with a selected material by preparing simple blends,[10] interpenetrating networks (IPNs)[11–14] and postpolymer modifications like crosslinking and surface modification.[15–17] Most polymers, despite having competitive selectivity, are susceptible to plasticization effects when used in industrial applications for separations of CO_2/N_2, CO_2/CH_4, propylene/propane and many other gases.[18–20] The plasticization is much more pronounced when the membrane is used for gaseous mixtures where CO_2 is one of the components. Hence, it is highly desirable to prepare stable membrane materials with high selectivity. Generally,

Correspondence to: A. Kumar (ashwani.kumar@nrc-cnrc.gc.ca).

annealing,[21] crosslinking,[22] IPN formation,[23] polymer blending,[24] and hyperbranched polymers[25] have been reported to suppress plasticization.

According to IUPAC,[26] interpenetrating polymer network (IPN) is a polymer comprising two or more networks, which are at least partially interlaced on a molecular scale but not covalently bonded to each other and cannot be separated unless chemical bonds are broken. Semi-IPN is also a polymer comprising one or more networks and one or more linear or branched polymer(s) characterized by the penetration on a molecular scale of at least one of the networks by at least some of the linear or branched macromolecules.[27] Recently, our lab reported semi-IPNs from polyether sulfone and polyether imides as the linear, nonreactive polymer and the bismaleimide as the reactive constituent forming the crosslinked network.[11–14] We found that *in situ* polymerization of BMI monomer inside PEI/NMP solution forms hard phase of thermoset BMI resin that interpenetrates soft phase of thermoplastic polyether imide (PEI) networks, i.e., formation of physical interlock between the two phases leading to polymeric nano-scale multidomain blends having extraordinary properties. These semi-IPN membranes gave 15 times higher gas flux than those membranes prepared from pure PEI without significant decrease in gas selectivity.[11–14]

Polyethylene glycol (PEG) based polymers are shown to exhibit good CO_2 separation characteristics owing to solubility of CO_2 in polar PEG.[9] Polyimides having PEG soft segments are reported where the hard polyimide segments render the stability and the soft PEG segments account for the high selectivity.[28] These materials are prepared by copolymerizing the aminopropyl terminated PEG with dianhydride and aromatic amines. The IPN of commercial PEI and poly (ethylene glycol) diacrylate (PEGDA) will be cost effective than the tailor made polymers and also expected to have other desirable properties.

The efficiency of polymeric gas separation membranes is often expressed as the material's pure gas permeability coefficient and its ideal permselectivity.[5] Because these are basically material properties, once the polymer has been chosen, the membrane productivity can be improved by reducing the thickness with out surface defects. The phase inversion process developed by Loeb and Sourirajan[29] offers the best way to produce integrally skinned asymmetric membranes with a very thin skin layer and a porous support layer. The skin layer determines both the permeability and selectivity of the membrane, whereas the porous substructure functions primarily as a physical support for the skin. The asymmetric membranes can be made as flat sheet membranes or hollow fiber membranes. The asymmetric membranes are predominantly used in industrial applications because of higher permeation than the dense membranes. The study of asymmetric membranes gives a better picture of its commercial usefulness. However, development of thin-skinned asymmetric membranes would result in defects or pinholes on skin surface because of irregular packing of kinked polymer chains and incomplete coalescence of polymer molecules in skin layer.[30] Therefore, silicone-coated membranes are commonly utilized in industrial membrane gas separation processes.[11–14] This technique is used to repair any defects or pores which may occur in the active layer of a gas separation membrane. Blocking these cavities will result in a decrease in convective flow but improvement on selectivity. This post treatment allows the membrane to display permeation properties closer to the inherent characteristics of the membrane polymer itself while improving the selectivity for gas pairs.

In this article we report the semi-IPNs prepared from commercial PEI polymer and PEGDA. It is expected that PEG molecules will render increased solubility selectivity for CO_2/N_2, and the PEI will provide the required stability to the semi-IPN material. The variation in the properties with increasing amounts of PEGDA content is studied in detail, to identify the best material composition. Gaseous separation properties of the asymmetric membranes prepared from the semi-IPN material are also reported.

EXPERIMENTAL

Materials

Aromatic PEI ULTEM® 1000 was supplied by General Electric Plastics, (USA) in pellet form and was dried in an oven at 150°C for 8 h before use to remove any moisture. Anhydrous 1-methyl-2-pyrrolidinone (NMP), (Aldrich) 99.5% reagent grade (water < 0.005%), PEGDA (Mol.Wt. 700) and Benzophenone were supplied by Sigma-Aldrich (Canada). Anhydrous ethyl alcohol was received from Commercial Alcohols (Ontario, Canada). Hexanes of ACS reagent grade were supplied by VWR (Canada). All solvents were used as supplied under a dry nitrogen atmosphere. Ultra high purity medical air, CO_2, and Industrial grade Nitrogen were supplied by BOC Gases (Canada) and were used as received without further purification.

Synthesis of polyether imide and PEGDA semi-IPN membranes

The known quantity (cf. Table I) of commercial polyether imide was first dissolved in NMP by rolling

TABLE I
Compositions of Formulations for Making Membranes

S.No	Membrane code	PEI (g)	PEGDA (g)	Initiator (g)	NMP (mL)	PEGDA (wt %)
1	PEI	25	0	0	80	0
2	PEI-PEGDA (1.9%)	25	0.5	0.03	80	1.9
3	PEI-PEGDA (3.8%)	25	1.0	0.03	80	3.8
4	PEI-PEGDA (5.7%)	25	1.5	0.03	80	5.7
5	PEI-PEGDA (7.4%)	25	2	0.01	80	7.4
6	PEI-PEGDA (13.8%)	25	4	0.03	80	13.8
7	PEI-PEGDA (19.4%)	25	6	0.06	80	19.4
8	PEI-PEGDA (24.2%)	25	8	0.09	80	24.2
9	PEI-PEGDA (28.6%)	25	10	0.15	80	28.6

the bottle of each sample at 60°C. After the polyether imide was completely dissolved, calculated amount of PEGDA and the photo-initiator benzophenone was added into the solution. Then the mixture was rolled at room temperature and noted that the transparency of the solutions disappeared, and the solution became turbid with time. The complete disappearance of transparency indicated the completion of crosslinking, which was experimentally confirmed by Fourier Transform Infra Red (FT-IR). As soon as the turbidity appeared, the membranes were cast at room temperature on clean glass plates placed in a glove box equipped with a gas filter. After casting each sample with a doctor knife having a gap of 250 μm, the plate was quickly immersed in distilled water at ambient temperature. The membrane films were left in water for 3 days, which was frequently changed then washed and stored in anhydrous ethanol bath for 1 day. Membranes were subsequently placed in hexanes for 1 day before leaving them in a fume hood for 1 day. Drying was carried out at 80°C in air purging convection oven for 1 day and finally in vacuum oven at 80°C and 96.7 kPa (725 mmHg) for 2 days. Three circular coupons of 7.4×10^{-2} m diameter were cut from each sample to be used in the permeation test whereas the remaining material was used for thermal, microscopic, and spectroscopic characterizations. The coupons of the membranes used in the permeation test were coated with silicon rubber. A solution of 3% Sylgard 184 with a catalyst to base rubber ratio of 1 : 10 in *n*-pentane was sprayed as a thin layer on the top surface of the membrane and the solvent was allowed to evaporate. Application of four coatings was found to be adequate for making gas separation membranes. Finally, the silicon coated membranes were cured in air purging convection oven at 80°C for 1 day. Reproducibility of the gas permeation values of the membrane was found to be ±2% in most cases.

Measurements

Fourier transform infrared attenuated total reflection (FTIR-ATR) analysis was performed using a Super Charged ZnSe single-bounce ATR crystal with a tensor FT-IR spectrometer (Bruker IFS 66). The spectra were taken with 200 scans at a resolution of 4 cm^{-1} in the range of 400–4000 cm^{-1}. The FT-IR-ATR background was performed at the same conditions without a sample in place. A Thermal Analysis (TA) instrument model 2920 Modulated Differential Scanning Calorimetry (DSC), calibrated with Indium at 156.5985°C and with Tin at 231.93°C was used to measure the glass-transition temperature (T_g). Under a nitrogen atmosphere, polymer samples were ramped to 250°C at 5°C/min. The T_g was calculated at the point of inflection of the DSC curve. TA instruments, Model AutoTGA 2950 analyzer was used for measuring the degradation temperatures by thermogravimetric analysis (TGA). Under a nitrogen atmosphere, polymer samples were heated to 120°C at 10°C/min, and were held isothermally for 60 min to remove moisture, if any, cooled and isothermally kept at 40°C, before heating to 1000°C at the rate of 10°C/min.

The morphology of the membrane samples without silicon rubber coating were examined by scanning electron microscope (SEM) using JEOL 840A equipment at an accelerating voltage of 10 kV. Samples were prepared by cutting a strip from membrane, freezing in liquid nitrogen, and fracturing to obtain a representative sample. They were mounted on carbon tape at 45° SEM stubs and sputter coated with gold. Photographs were taken at different magnifications.

A cross-flow test cell having a permeation surface area of 9.6 cm^2 was used. Pure O_2, N_2, and medical air were used to study O_2/N_2 separation. Pure CO_2, N_2 were used to study ideal CO_2/N_2 selectivity. Feed pressure of 665 kPa gauge (498.8 cmHg) was used and the retentate was set at a flow rate of 6.6×10^{-6} m^3(STP) s^{-1} whereas permeate was discharged to atmosphere. The permeate flow rate was measured by a soap bubble flow meter, and O_2 concentration of feed and permeate gas mixtures were determined by Oxygen Sensor (Quantek Instruments Oxygen/Carbon dioxide analyzer Model 902P). All membranes were conditioned for 2 h in each gas before taking the measurements.

RESULTS AND DISCUSSION

Synthesis and spectral analysis of polyether imide and PEGDA semi-IPN membranes

In continuation of our efforts to synthesis novel polymer membranes[11–14] for gas separation applications, here we report the synthesis and characterization of PEI-PEGDA semi-IPNs. The semi-IPNs are synthesized with PEI as the nonreactive backbone. PEGDA was used as the reactive constituent. PEGDA was crosslinked in presence of PEI to get semi-IPNs. Scheme 1 gives the schematic representation of the synthesis of semi-IPN membranes.

Table I lists the composition used to synthesize semi-IPN membranes. Several crosslinking methods were tried to identify the best suitable procedure for making the gas separation membranes. Initially, the polyether imide solution, mixed with the PEGDA and a thermal initiator (benzoyl peroxide) was casted on a glass plate, which was subsequently sandwiched between two glass plates with a silicone sealant to avoid the interference of the moisture and to avoid the evaporation of the solvent thus forming dense or symmetric membranes. These membranes did not give good gas permeation properties because of the condensation of solvent on the surface leading to defective top layer, and also the morphology analysis indicated phase segregation. Alternatively, a similar polymer solution except for the use of photo-initiator instead of thermal initiator was casted and sandwiched between glass plates separated by a silicone sealant, which was exposed to UV irradiation. The semi-IPN membranes, prepared by exposing to UV radiation, formed phase separated structure leading to poor gas permeation properties. Based on our previous knowledge,[11–14] the green chemistry method was adopted. The polymer solutions with PEGDA and a calculated amount of photo-initiator were run in the rollers at room temperature and monitored for the completion of crosslinking. The

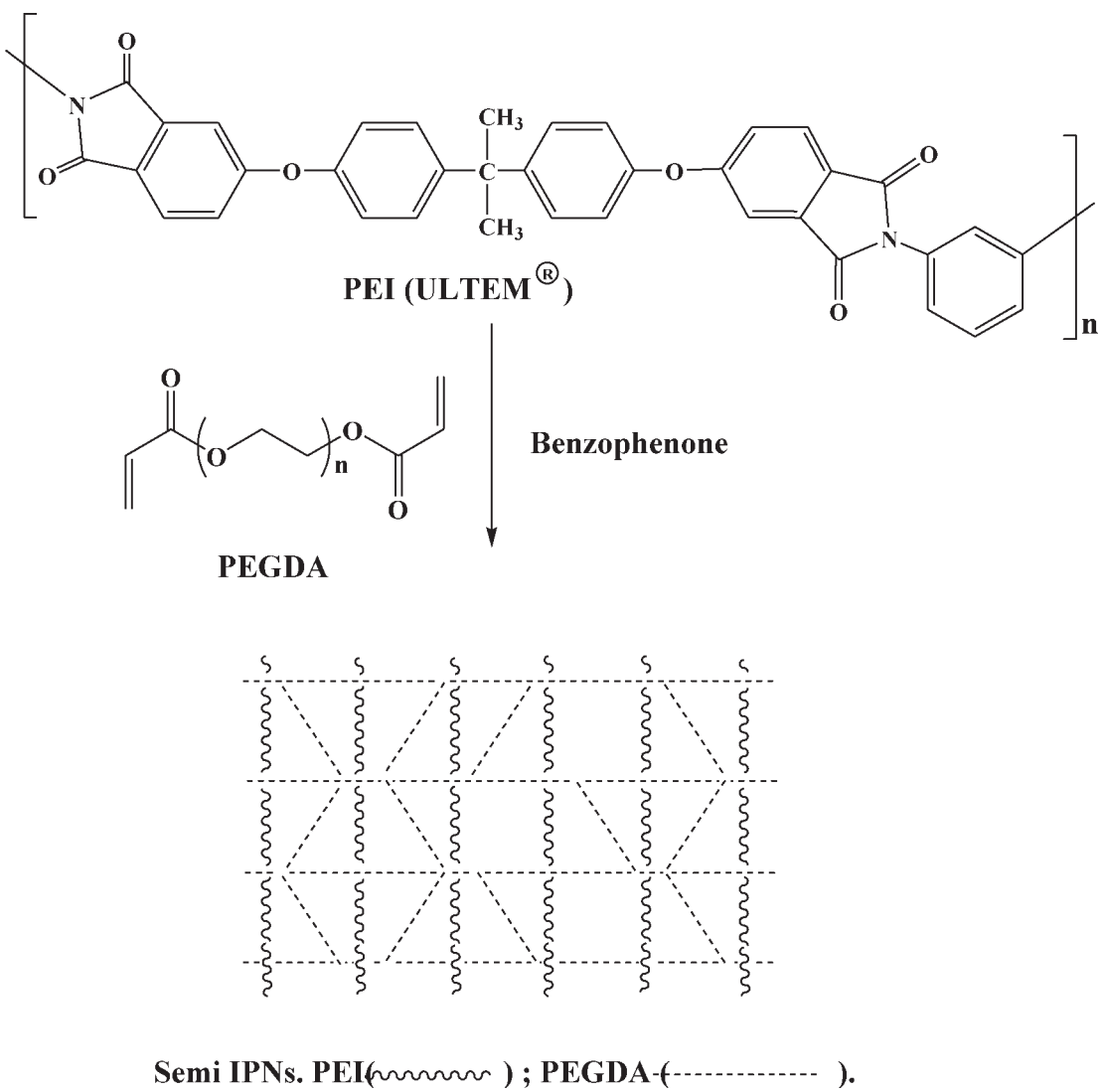

Scheme 1 Synthesis of PEI-PEGDA semi-IPNs.

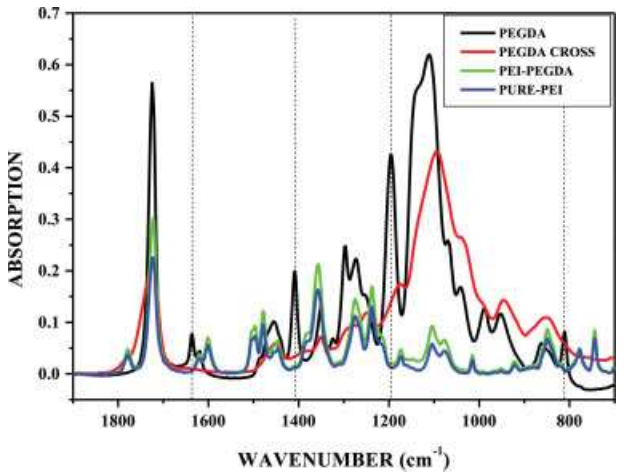

Figure 1 FT-IR spectra of PEGDA, PEGDA dense film and polymer membranes. [Color figure can be viewed in the online issue, which is available at www.interscience.wiley.com.]

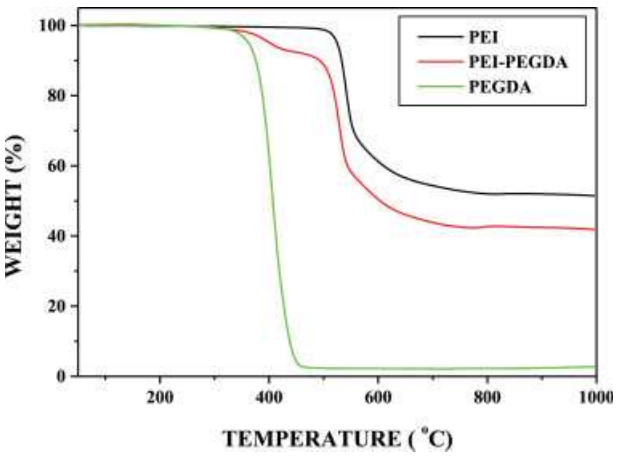

Figure 2 TGA thermograms of polymer membranes and PEGDA. [Color figure can be viewed in the online issue, which is available at www.interscience.wiley.com.]

complete disappearance of transparency indicated the completion of crosslinking, which was experimentally confirmed by FT-IR. The membranes were prepared as soon as there was complete disappearance of transparency or the solution became completely turbid. Additional processing even after the complete turbidity lead to precipitation of a polymer because of phase separation, as previously observed[11,31] and in case of higher PEGDA content (>13.8%) the solution completely solidified. The time taken for the appearance of turbidity depended on the amount of PEGDA, the reactive constituent. For the material with the highest PEGDA content in this study (28.6 wt %), the turbidity appeared rapidly (10 h), whereas the solutions having less PEGDA took longer time (4 days in case of 3.8 wt % of PEGDA). The amount of PEI was kept constant (25 g) in all the experiment whereas the amount of PEGDA was increased. We observed a variation in the viscosity if both PEI and PEGDA content were varied to keep the total weight constant. Considering that viscosity of the casting solution has been reported to affect the morphology and performance of the membrane,[32,33] the PEI amount was kept constant to maintain same viscosity. It was also observed that exceeding PEGDA above 28.6 wt % resulted in significant phase separation leading to poor membranes performance. The successful synthesis of the semi-IPNs and completion of crosslinking reaction of PEGDA was confirmed by FT-IR-ATR which is given in Figure 1. The figure includes PEGDA, a dense film from crosslinked PEGDA, PEI and PEI-PEGDA membranes. All the characteristic acrylic absorptions (1640, 1409, 1190, 810 cm^{-1})[34] shown in the figure are highlighted with dotted line, which disappeared in the PEGDA crosslinked dense film (PEGDA CROSS) and PEI-PEGDA semi-IPNs as well. This confirms the consumption of acrylic double bonds leading to the successful formation of the semi-IPN. The characteristic imide carbonyl stretching vibrations were exhibited at 1780 cm^{-1} (symmetric) and 1722 cm^{-1} (asymmetric). The ester carbonyl absorption of PEGDA found to overlap with the asymmetric stretching of the imide carbonyl group. The absorption of aromatic ether group (Ar—O—Ar) was observed at 1240 cm^{-1} and absorption of the C—N—C of the imide ring was observed at 1357 cm^{-1}. The presence of the imide absorptions confirmed that the PEI is indeed intact.

Thermal properties of the semi-IPN membranes

The thermal stability of the semi-IPN membranes, PEI and a PEGDA dense film was measured with thermogravimetric analyzer and the TGA results are presented in Figures 2 and 3. The polymer samples

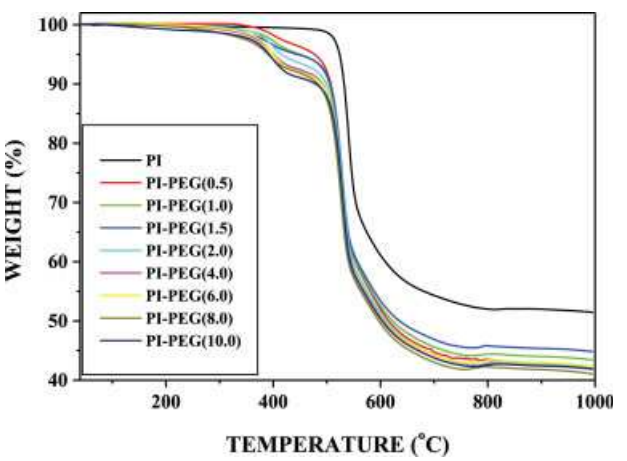

Figure 3 TGA thermograms of polymer membranes. [Color figure can be viewed in the online issue, which is available at www.interscience.wiley.com.]

TABLE II
Thermal Properties of Semi-IPN Membranes

Polymer	Onset temperature (°C) First step	Onset temperature (°C) Second step	5% Weight loss	Residue (%) at 990 °C
PEI	521.2		522.6	50.9
PEI-PEGDA (1.9%)	357.9	496.7	475.9	42.2
PEI-PEGDA (3.8%)	358.3	497.7	447.8	43.4
PEI-PEGDA (5.7%)	359.5	497.6	441.8	44.9
PEI-PEGDA (7.4%)	364.3	503.3	414.2	42.1
PEI-PEGDA (13.8%)	366.9	498.3	402.7	42.1
PEI-PEGDA (19.4%)	367.8	500.5	399.1	42.3
PEI-PEGDA (24.2%)	356.5	492.9	388.1	40.9
PEI-PEGDA (28.6%)	362.3	496.9	391.9	41.9
PEGDA	371.0		359.0	1.9

were conditioned at 120°C for 1 h in the TGA to avoid the interference of moisture. Figure 2 gives the thermograms of pure PEI, PEGDA dense film and PEI-PEGDA semi-IPN membranes. It can be seen that the first step degradation resembles that of the PEGDA dense film and the second step resembles that of PEI. It is understood from the Figure 3 that all PEI-PEGDA semi-IPN membranes followed two-step degradation patterns. The onset of first step degradation was around 360°C. In the present PEI-PEGDA semi-IPN membranes, the first stage degradation might be due to the degradation of thermally labile PEG groups as inferred from the Figure 2. The onset degradation temperature, 5% weight loss temperature and the residual weight are tabulated in Table II. One can observe from Table II that the onset of first step degradation temperature showed slightly increasing trend with increase in the PEGDA content. Also the percentage of weight loss in the first step increased (Fig. 3) and 5% weight loss temperature decreased with increase in PEGDA content. This again confirms the successful incorporation of PEGDA forming the desired PEI-PEGDA interpenetrated network. The second step indicated the decomposition of the polyether imide backbone. Although it was expected that interpenetrating network formation will increase the thermal stability, the second step showed almost similar degradation temperature. This is because PEG group has lower thermal stability than that of polyether imide backbone leading to disintegration of the network structure even before the polyether imide started degrading. Hence, interpenetrating networks did not have a pronounced effect on the decomposition in the second step. The residual weight is higher in the case of PEI and it decreased with the semi-IPNs. This must be because of the presence of labile PEG groups present in the given weight of the membrane. Although the overall stability of semi-IPNs is slightly lower than the PEI (cf. Table II, 5% weight loss temperature), still the semi-IPN membranes exhibited sufficient stability to find use in industrial applications.

The glass transition temperature (T_g) of the PEI, PEGDA dense film and PEI-PEGDA semi-IPN membranes were measured by DSC and a representative thermogram is given in Figure 4(a,b, and c). The T_g

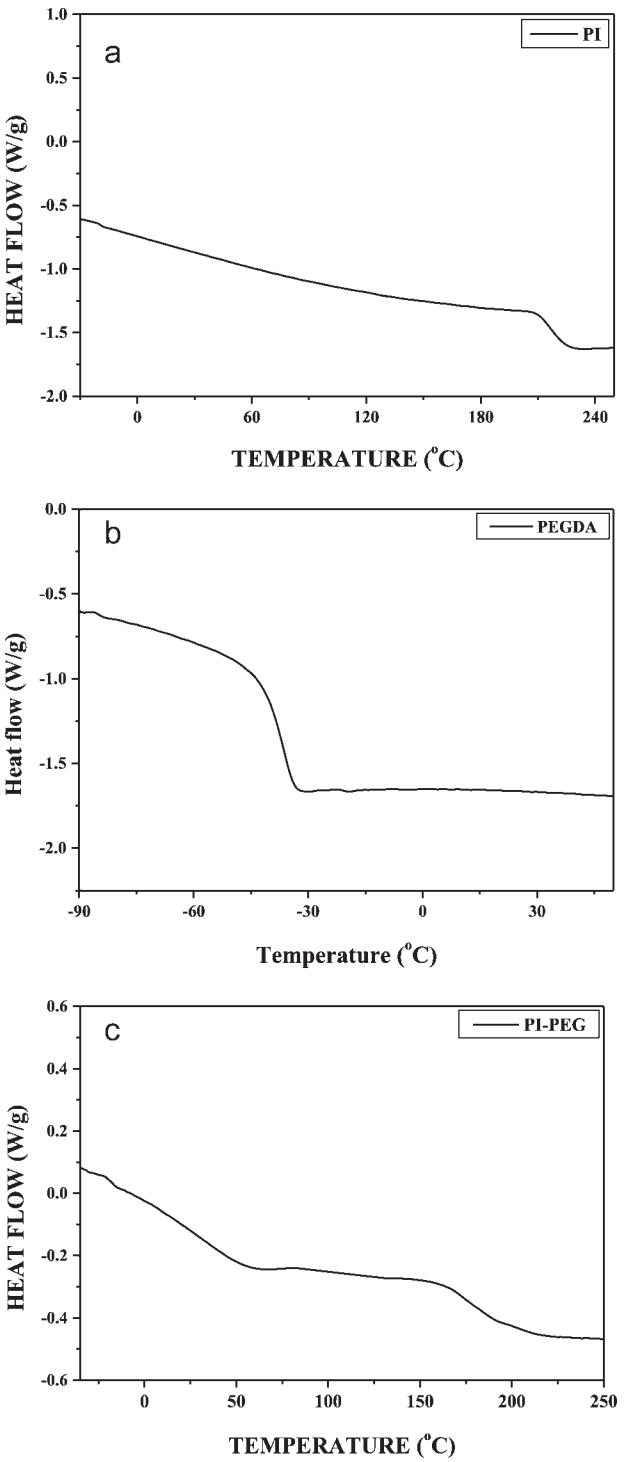

Figure 4 (a) DSC thermograms of PEI membrane. (b) DSC thermograms of PEGDA dense film. (c) DSC thermograms of PEI-PEGDA semi-IPN membrane.

of the pure polyether imide is 210°C, which agrees with previously reported values.[12] As can be seen from the Figure 4(a) that the T_g of the PEI is very distinctive and the transition is mostly suppressed in the semi-IPNs [Fig. 4(c)] indicating the formation of network structure. Also it can be seen from Figure 4(c) that the T_g transition of the semi-IPNs occurs at a wide temperature range indicating the increased rigidity of the polymer chains owing to IPN formation. A minor transition at –17°C, which may be due to the PEG segment is also seen. A dense film of crosslinked PEGDA was prepared and was analyzed by DSC [Fig. 4(b)]. The characteristic T_g transition was observed at –36°C, which is closely related to the reported value (–40°C).[35] The increase in the T_g transition of the PEGDA in the semi-IPNs may be because of the rigid network formation and the influence of PEI. It can be further noticed that the T_g of the polyether imide segment in the semi-IPN [Fig. 4(c)] has shifted to lower temperature range. This might be due to the plasticization effect of the PEG. This kind of plasticization effect of one of the constituents in the semi-IPN was observed earlier.[12,36] Because the membranes are semi interpenetrated network, the polymers were able to exhibit transition owing to the individual components of the IPNs. This also proves the formation of semi-IPNs of the polyether imide and PEGDA. Generally, lower glass transition indicates the flexible nature of the polymer chains and is expected to increase the permeation and decrease the selectivity. This may also be a reason for high permeation and low selectivity of semi-IPNs having high PEGDA content, which will be discussed in gas permeation studies.

Membrane morphology

Membrane morphology plays an important role in determining membrane performance for gas separations. Surfaces of all membrane samples were initially screened by optical microscope for the presence of phase separation. Obvious phase separations were observed for membranes having more than 28.6 wt % of PEGDA content. These membranes did not exhibit good gas permeation properties. The phenomenon of phase separation was found to influence the membrane performance for gas separation by earlier studies with PEI/BMI based semi-IPNs.[11–14] Morphology of membranes was examined by SEM and representative micrographs, which are presented in Figure 5(a,b, and c). Figure 5(a) gives the cross section view of PEI membrane. Figure 5(b) gives the cross section view of PEI-PEGDA (5.7%) membrane, which has highest CO_2/N_2 selectivity in this series. Figure 5(c) gives the cross section view of PEI-PEGDA (28.6%) membrane, which has the highest PEGDA content. The

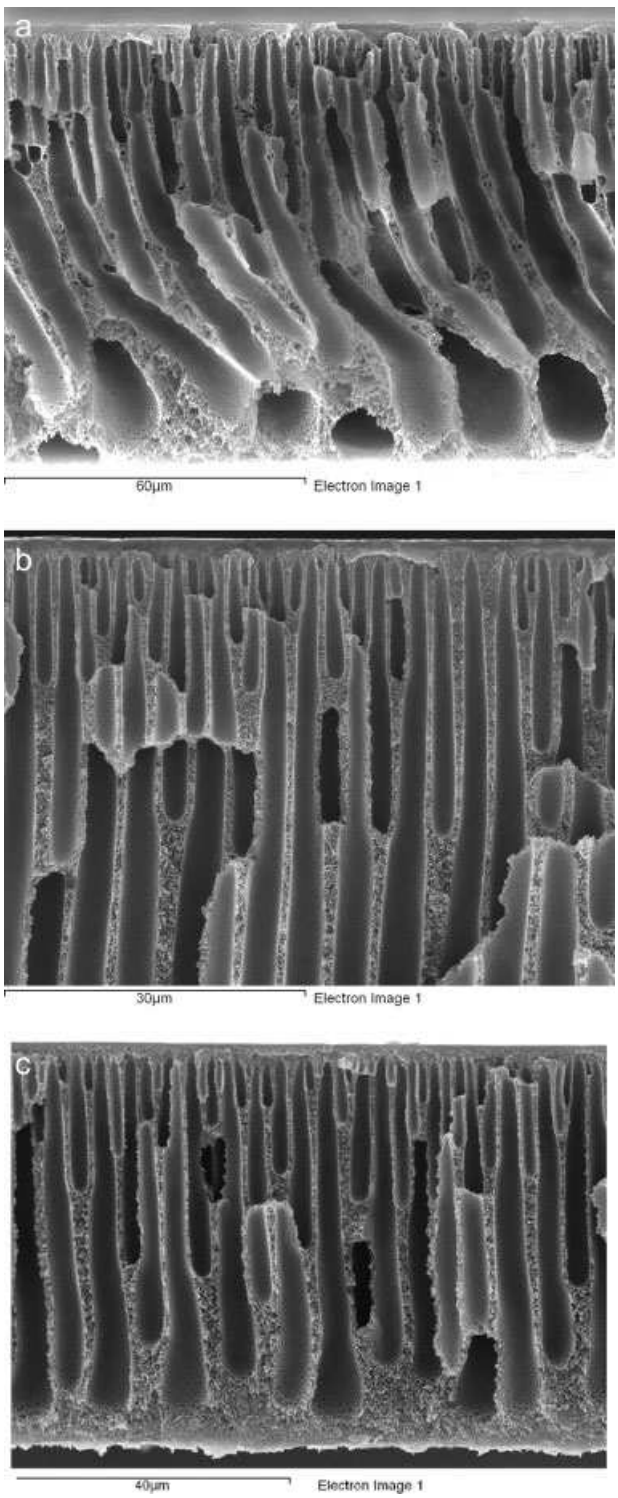

Figure 5 (a) Scanning electron micrographs of PEI membrane. (b) Scanning electron micrographs of PEI-PEGDA (5.7%) membrane. (c) Scanning electron micrographs of PEI-PEGDA (28.6%) membrane.

cross section SEM micrographs of the semi-IPNs presented in Figure 5(a,b and c) revealed that all of these membranes exhibited characteristic morphology of asymmetric membranes consisting of a dense top layer and a porous sublayer.[37] All the semi-IPN

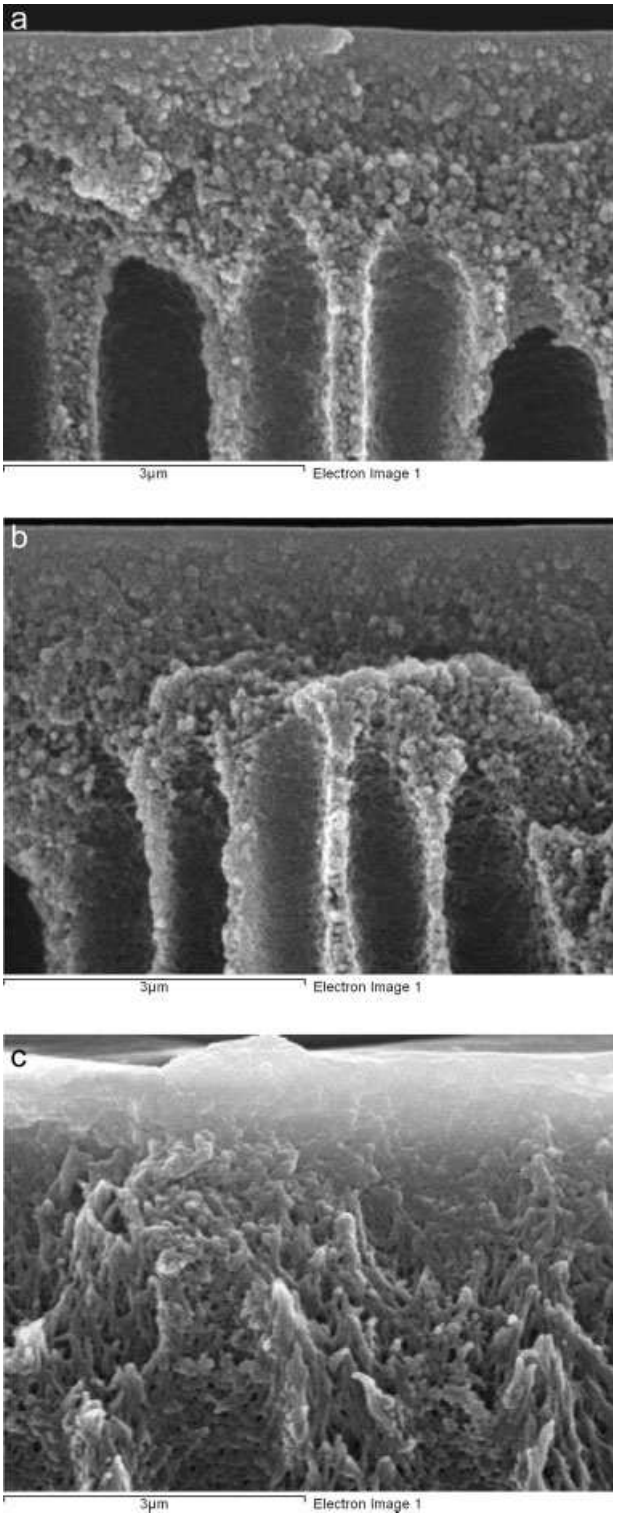

Figure 6 (a) Scanning electron micrographs of PEI-PEGDA (1.9%) membrane. (b) Scanning electron micrographs of PEI-PEGDA (5.7%) membrane. (c) Scanning electron micrographs of PEI-PEGDA (28.6%) membrane.

membranes exhibited conical voids and the spherical voids were very scarce compared to pure PEI [Fig. 5(a)]. The finger-like conical porous structure was present in all the membranes. The morphological structure was influenced by the membrane material, solution compositions, and gellation conditions, as discussed in previous reports.[11–14] The micrographs (5a) (5b) and (5c) clearly show that the porous finger-like structures penetrated all along cross section perpendicular to membrane surface. The fingers have a relatively small diameter at the top, which increase along the length. The fingers were uniformly formed throughout the membrane at almost equal distances indicating the similar morphology in the sub layer of the semi-IPN membranes [Fig. 5(b,c)], whereas many of them are disrupted and not going all along the cross section in the PEI membrane [Fig. 5(a)]. With increase in the PEGDA content, the membrane showed slightly different morphology as shown in Figure 6(a,b, and c). Figure 6(a,b, and c) give the magnified image of the selective top layer and subsequent support layer of the semi-IPN membranes PEI-PEGDA (1.9%), PEI-PEGDA (5.7%) and PEI-PEGDA (28.6%), respectively. Although the finger-like structure was formed in the same way in all of these membranes, the porosity at the top and bottom of support layer significantly changed. With higher PEGDA content [Fig. 6(c)] the porosity increased, compared with lower concentrations [Fig. 6(a,b)], which can be seen from the higher magnification of the top section of support layer. This must be the result of increase in hydrophilicity of the membrane with increase in PEGDA content. Similar effects have been observed in PES/PEG blends for ultrafiltration membranes.[38] There is no apparent difference in the top and bottom layer thickness or the density of the finger-like structure.

Gas permeation studies

The novel PEI-PEGDA semi-IPN membranes were tested for gas permeation properties and presented in Tables III–V. The pure gas permeance of O_2, N_2,

TABLE III
Air Permeation Properties of Semi-IPN membranes

S.No	Membrane	Permeance GPU[a]		Selectivity O_2/N_2
		Air	O_2	
1	PEI-PEGDA (1.9%)	1.7	1.3	3.2
2	PEI-PEGDA (3.8%)	1.5	1.2	4.3
3	PEI-PEGDA (5.7%)	1.1	0.9	3.8
4	PEI-PEGDA (7.4%)	3.1	2.5	4.3
5	PEI-PEGDA (13.8%)	1.8	1.4	3.4
6	PEI-PEGDA (19.4%)	3.6	2.6	2.9
7	PEI-PEGDA (24.2%)	31.7	21.6	2.2
8	PEI-PEGDA (28.6%)	83.6	54.6	1.9
9	PEI	1.10	0.83	3.15

[a] Gas permeation unit. GPU $= 1 \times 10^{-6}$(cm^3 (STP)/cm^2 s cmHg.

CO_2 were determined. The ideal selectivities of O_2/N_2 and CO_2/N_2 were calculated from the permeance of pure gases and presented in Table IV and V. Also the O_2 enrichment of the air was evaluated and the O_2/N_2 selectivity was calculated as in previous reports[11–14] and given in Table III. It can be noted that performance of the synthesized semi-IPN membranes were different based on the ideal selectivity calculated from pure gases, O_2 and N_2 and the selectivity obtained from the air. The ideal selectivity in the case of O_2/N_2 (cf. Table IV) was higher than the observed selectivity from air (cf. Table III). Also the performance of the membranes was different for different pair of gases. The membrane showing better O_2/N_2 (cf. Table IV) selectivity did not exhibit higher CO_2/N_2 selectivity (cf. Table V). This may be because the PEG groups affects the solubility selectivity of CO_2/N_2 whereas, it do not have pronounced effect on the O_2/N_2 selectivity. Based on the pure gas permeation studies, the overall performance (for both O_2/N_2 and CO_2/N_2 selectivity) of the membranes was better with the lower PEGDA content. When the PEGDA content increased from 1.9 to 5.7%, there was an appreciable change in the ideal selectivity. The selectivity peaked at 3.8% of PEGDA for O_2/N_2 (cf. Table IV) and 5.7% of PEGDA for the CO_2/N_2 (cf. Table V). With further increase in the PEGDA content up to 19.4%, the selectivity kept decreasing slowly without a relative change in the permeance. Above the 19.4% of PEGDA, there was a substantial increase in the flow with a noticeable drop in the selectivity. As discussed in membrane morphology, the increase in the porosity of the membrane at higher PEGDA content should be the reason for the observed trend. The increase in PEGDA content was expected to increase the CO_2 permeance, selectively, because of the polar nature of the PEG. In many of the dense films, there appears to be a monotonous relation with the PEG content and CO_2 permeance independent of the method of preparation.[3,34] Both the physical blends with PEG and PEG incorporated polymers showed the above trend.[38,39]

TABLE IV
Oxygen and Nitrogen Permeation Properties of Semi-IPN Membranes

S.No	Membrane	Permeance GPU[a] O_2	Permeance GPU[a] N_2	Selectivity O_2/N_2
1	PEI-PEGDA (1.9%)	1.5	0.4	4.2
2	PEI-PEGDA (3.8%)	1.4	0.3	5.8
3	PEI-PEGDA (5.7%)	1.0	0.2	5.7
4	PEI-PEGDA (7.4%)	2.6	0.5	5.0
5	PEI-PEGDA (13.8%)	1.6	0.4	4.0
6	PEI-PEGDA (19.4%)	2.3	0.7	3.1
7	PEI-PEGDA (24.2%)	16.4	9.2	1.8
8	PEI-PEGDA (28.6%)	56.9	27.5	2.1
9	PEI	1.26	0.17	7.2

[a] Gas permeation unit. GPU $= 1 \times 10^{-6}$(cm^3 (STP)/cm^2 s cmHg.

TABLE V
Carbon-di-oxide and Nitrogen Permeation Properties of Semi-IPN Membranes

S.No	Membrane	Permeance GPU[a] CO_2	Permeance GPU[a] N_2	Selectivity O_2/N_2
1	PEI-PEGDA (1.9%)	10.9	0.4	29.4
2	PEI-PEGDA (3.8%)	9.3	0.3	37.1
3	PEI-PEGDA (5.7%)	8.8	0.2	48. 8
4	PEI-PEGDA (7.4%)	13.2	0.5	25.9
5	PEI-PEGDA (13.8%)	9.3	0.4	23.8
6	PEI-PEGDA (19.4%)	11.2	0.7	15.1
7	PEI-PEGDA (24.2%)	130.4	9.2	14.2
8	PEI-PEGDA (28.6%)	199.6	27.5	7.3
9	PEI	3.45	0.17	19.81

[a] Gas permeation unit. GPU $= 1 \times 10^{-6}$(cm^3 (STP)/cm^2 s cmHg.

The asymmetric membranes, however, did not show the above trend. Although the PEG incorporated membranes showed better performance for CO_2/N_2 than the O_2/N_2, there was no monotonous relation with the PEGDA content, and also the selectivity was lower than expected from dense films. The increase in the PEGDA content affects the material in two ways. At a higher content of PEG groups the thermodynamic incompatibility between the PEI and PEG will increase resulting in phase segregation. With higher phase segregation the surface defects may increase leading to poor performance of the membrane. Also with increase in the PEGDA content, the inherent hydrophilicity of the material increases. When the membranes were gelled by immersing in the water, the phase inversion occurs rapidly leading to highly porous structure as indicated in morphological analysis. This leads to the tradeoff in gas permeation and selectivity of the material. All the semi-IPN membranes in the present work showed remarkable stability to CO_2 exposure and no plasticization was observed. Even after 24 h exposure to CO_2 at 100 psi, the membranes recovered within 10 min by permeating nitrogen.

The results prove that the incorporation of polar PEG groups to improve CO_2/N_2 selectivity can be accomplished by preparing semi-IPN membranes. The semi-IPN membranes exhibited mechanical robustness, higher thermal stability than the PEGDA dense film, and also the asymmetric membranes can be conveniently made, which would be difficult with pure PEGDA based materials. As a synergic property, the PEG groups rendered higher CO_2/N_2

selectivity to the semi-IPN membranes. Based on the performance, a proper composition of PEI/PEGDA will be selected and membranes will be prepared by varying the preparation conditions to get better permeance without compromising on the selectivity.

CONCLUSIONS

The semi-IPNs could be formed from PEI (ULTEM®) and PEGDA and their formations were confirmed by the absence of acrylic double bonds in the FT-IR. Based on the two step degradation pattern in TGA, the PEG groups were believed to be incorporated into polyether imide. The increase in the percent weight loss of the first step with increase in PEGDA content indicated that increasing amount of PEG group was incorporated into the semi-IPN membranes. The SEM micrographs revealed the change in morphology with change in PEGDA content. The increase in the porous morphology with increase in PEGDA content underlined the relationship between the gas permeation and membrane morphology. A tradeoff between the permeation and selectivity is observed with increasing content of PEGDA and at a 5.7 wt % of PEGDA, highest CO_2/N_2 selectivity was observed. The change in gaseous separation properties with increase in PEGDA content was not monotonous relation and can be clearly understood by looking at different region. In the first region where the PEGDA wt % increased from 1.9 to 5.7%, the ideal selectivity for CO_2/N_2 increased with out much change in permeance of pure gases. In the second region where the PEGDA wt % increased from 7.4 to 19.4%, the selectivity decreased with out appreciable change in the permeance. In the third region where the PEGDA wt % increased from 24.2 to 28.6%, the selectivity decreased and there was significant increase in the permeance indicating the porous nature of the selective layer. In light of the current work, a suitable composition (PEI-PEGDA 5.7%) should be modified by changing the initial viscosity and other membrane making techniques to obtain higher permeation leading to better performance.

The authors are thankful to Mr. David Kingston for the SEM experiments and Mr. Gilles Robertson for his advises on analyzing thermal properties.

References

1. Baker, R. W. Membrane Technology and Applications, 2nd ed.; Wiley: Chichester, 2004.
2. Baker, R. W. Ind Eng Chem Res 2002, 41, 1393.
3. Powell, C. E.; Qiao, G. G. J Membr Sci 2006, 279, 1; and references therein.
4. Pandey, P.; Chauhan R. S. Prog Polym Sci 2001, 26, 853.
5. Stern, S. A. J Membr Sci 1994, 94, 1.
6. Robeson, L. M. Curr Opin Solid State Mat Sci 1999, 4, 549.
7. Smid, J.; Albers, J. H. M.; Kusters, P. M. J Membr Sci 1991, 64, 121.
8. Wind, J. D.; Paul, D. R.; Koros, W. J. J Membr Sci 2004, 228, 227.
9. Barbari, T. A.; Koros, W. J.; Paul, D. R. J Polym Sci Part B: Polym Phys 1988, 26 709.
10. Sua, T. M.; Ballb, I. J.; Conklinc, J. A.; Huangb, S. C.; Larsonb, R. K.; Nguyenb, S. L.; Lewb, B. M.; Kanerb, R. B. Synth Met 1997, 84, 801.
11. Kurdi, J.; Kumar, A. J Appl Polym Sci 2006, 102, 369.
12. Kurdi, J.; Kumar, A. J Membr Sci 2006, 280, 234.
13. Kurdi, J.; Kumar, A. Polymer 2005, 46, 6910.
14. Kurdi, J.; Kumar, A. Sep Purif Technol 2006, 53, 301.
15. Rezac, M. E.; Schoberl, B. J Membr Sci 1999, 156, 211.
16. Liu, Y.; Wang, R.; Chung, T. S. J Membr Sci 2001, 189, 231.
17. Lin, H.; Freeman, B. D. Macromolecules 2005, 38, 8394.
18. Wessling, M.; Lopez, M. L.; Strathmann, H. Sep Purif Technol 2001, 24, 223.
19. Zhou, C.; Chung, T.-S.; Wang, R.; Liu, Y.; Goh, S. H. J Membr Sci 2003, 225, 125.
20. Wind, J. D.; Sirard, S. M.; Paul, D. R.; Green, P. F.; Johnston, K. P.; Koros, W. J. Macromolecules 2003, 36, 6433.
21. Krol, J. J.; Boerrigter, M.; Koops, G. H. J Membr Sci 2001, 184, 275.
22. Wind, J. D.; Staudt-Bickel, C.; Paul, D. R.; Koros, W. J Ind Eng Chem Res 2002, 41, 6139.
23. Bos, A.; Punt, I. G. M.; Wessling, M.; Strathmann, H. J Polym Sci B: Polym Phys 1998, 36, 1547.
24. Bos, A.; Punt, I. G. M.; Strathmann, H.; Wessling, M. Am Inst Chem Eng J 2001, 47, 1088.
25. Fang, J. H.; Kita, H.; Okamoto, K. J Membr Sci 2001, 182, 245.
26. Jenkins, A. D.; Kratochvfl, P.; Stepto, R. F. T.; Suter, U. W. Pure Appl Chem 1996, 68, 2287.
27. Sperling, L. H. Interpenetrating Polymer Networks and Related Materials; Mir: Moscow, 1984.
28. Yoshino, M.; Ito, K.; Kita, H.; Okamoto, K.-I. J Polym Sci Part B: Polym Phys 2000, 38, 1707.
29. Loeb, S.; Sourirajan S. Adv Chem Ser 1962, 38, 117.
30. Pinnau, I.; Koros, W. J. J Appl Polym Sci 1992, 46, 1195.
31. Gaina, V.; Gaina, C.; Stoleriu, A.; Timpu, D.; Sava, M.; Rusu, M. Polym Plast Technol Eng 1999, 38, 927.
32. Jansen, J. C.; Buonomenna, M. G.; Figoli, A.; Drioli, E. Desalination 2006, 193, 58.
33. Ismail, A. F.; Lai, P. Y. Sep Purif Technol 2003, 33, 127.
34. Lin, H.; Kai, T.; Freeman, B. D.; Kalakkunnth, S.; Kalika, D. S. Macromolecules 2005, 38, 8381.
35. Lin, H.; Wagner, E. V.; Swinnea, J. S.; Freeman, B. D.; Pas, S. J.; Hill, A. J.; Kalakkunnath, S.; Kalika, D. S. J Membr Sci 2006, 276, 145.
36. Liou, H.-C.; Ho, P. S.; Tung, B. J Appl Polym Sci 1998, 70, 261.
37. Pinnau, I.; Wind, J.; Peinemann, K. V. Ind Eng Chem Res 2028 1990, 29.
38. Wang, Y. Q.; Su, Y.-L.; Ma, X.-L.; Sun, Q.; Jiang, Z.-Y. J Membr Sci 2006, 283, 440.
39. Okomotto, K. I.; Umeo, N.; Okamyo, S.; Tanaka, K.; Kita, H. Chem Lett 1993, 225.